Abnormal Thickening as well as Thinning of the Photoreceptor Layer in Intermediate Age-Related Macular Degeneration

Sam Sadigh,[1] *Artur V. Cideciyan,*[1] *Alexander Sumaroka,*[1] *Wei Chieh Huang,*[1] *Xunda Luo,*[1] *Malgorzata Swider,*[1] *Janet D. Steinberg,*[1] *Dwight Stambolian,*[2] *and Samuel G. Jacobson*[1]

Purpose. To investigate the relationship between photoreceptor layers overlying and adjacent to large drusen in intermediate nonneovascular AMD.

Methods. Patients with AMD ($n = 41$; aged 53–83 years) and elderly control subjects without eye disease ($n = 10$; aged 51–79 years) were studied with spectral-domain optical coherence tomography. Characteristics of large drusen ($\geq$125 μm) were measured and the thickness of photoreceptor laminae overlying drusen and in retinal regions neighboring the drusen were quantified.

Results. There were 750 large drusen in 63 intermediate AMD eyes studied. The width of the drusen sampled averaged 352 μm (SD = 153) and the height averaged 78 μm (SD = 31). There was significant reduction of the photoreceptor outer nuclear layer (ONL) thickness overlying 92% of the drusen. The thickness of the layer corresponding to photoreceptor inner and outer segments above drusen was also reduced, and the reduction was proportional to ONL thickness. In a substantial fraction (~20%) of normally laminated paradrusen locations sampled within ~300 μm of peak drusen height, ONL thickness was significantly increased compared with age and retinal location-matched normal values. Topographical analyses of the macula showed ONL thickening occurring in paradrusen regions as well as retinal locations distant from drusen.

Conclusions. Reductions in the photoreceptor laminae overlying drusen were detectable and this is consistent with histological studies revealing neuronal degeneration in AMD. ONL thickening in some macular areas of AMD eyes has not been previously reported and may be an early phenotypic marker for photoreceptor stress, as it has been speculated to be in hereditary retinal degenerations. (*Invest Ophthalmol Vis Sci.* 2013;54:1603–1612) DOI:10.1167/iovs.12-11286

AMD is the leading cause of central visual loss and blindness in elderly populations of the industrialized world.[1–5] Remarkable progress has occurred in recent years in the understanding of the complex genetic and environment interactions that impact AMD vulnerability (e.g., see Refs. 6–8). Therapies for the less common but visually more devastating neovascular form of AMD have made great strides,[9] whereas the more common chronic macular retinal degenerative (atrophic) form of AMD remains with limited therapeutic options.[3,10]

In parallel with studies leading to clinical trials of treatment for atrophic AMD should be advances in the way AMD is monitored by noninvasive methods. Well-known markers for early stages of atrophic AMD are drusen, extracellular deposits that form between Bruch's membrane (BrM), and the RPE. Drusen have been traditionally identified and viewed en face, whether by color photography, fluorescein angiography, or by clinical examination. Quantifying drusen and other abnormal fundus features by en face viewing has been one of the mainstays of classification schemes for AMD[11] and of assessing outcomes of various clinical trials (e.g., see Ref. 12). The microscopic details of drusen have historically been described through postmortem donor retinal histopathology.[4,13–15] The advent of optical coherence tomographic (OCT) cross-sectioning of the retina has added a further modality to the armamentarium of noninvasive assessment of the microscopic details of AMD (e.g., see Refs. 16–18).

The present work examines the relationship between drusen and the adjacent photoreceptor layer in intermediate nonneovascular AMD, defined as the stage demonstrating one or more large ($\geq$125 μm) drusen but without foveal geographic atrophy.[3] In the atrophic form of AMD, histopathological studies have demonstrated photoreceptor loss[13–15] and in the many published OCT images including drusen and outer neural retina, it is evident that there is an associated thinning of the photoreceptor outer nuclear layer (ONL). Quantitation of the relationship of drusen and photoreceptors has only occurred, however, in a limited number of noninvasive cross-sectional imaging studies.[19–21] Our analyses show that overlying drusen, there is photoreceptor cell layer reduction as well as disturbance of the inner and outer segments. Unexpected was the finding of ONL thickening in some AMD patient retinas, a result that is reminiscent of a predegenerative state of the ONL in monogenic retinal degenerations.[22–26]

From the [1]Scheie Eye Institute, Department of Ophthalmology, Perelman School of Medicine at the University of Pennsylvania, and the [2]Departments of Ophthalmology and Genetics, Perelman School of Medicine at the University of Pennsylvania, Philadelphia, Pennsylvania.

Supported by a grant from the Pennsylvania Department of Health to the University of Pennsylvania, Macula Vision Research Foundation, the Beckman Initiative for Macular Research, and the Foundation Fighting Blindness. AVC is a Research to Prevent Blindness Senior Scientific Investigator.

Submitted for publication November 11, 2012; revised December 12, 2012; accepted January 21, 2013.

Disclosure: **S. Sadigh**, None; **A.V. Cideciyan**, None; **A. Sumaroka**, None; **W.C. Huang**, None; **X. Luo**, None; **M. Swider**, None; **J.D. Steinberg**, None; **D. Stambolian**, None; **S.G. Jacobson**, None

Corresponding author: Artur V. Cideciyan, Scheie Eye Institute, University of Pennsylvania, 51 N. 39th Street, Philadelphia, PA 19104; cideciya@mail.med.upenn.edu.

METHODS

Subjects

All patients in the study had a clinical diagnosis of AMD, and were Caucasian from an Amish population in Pennsylvania.[27] Color fundus photos taken at screening sessions were reviewed and preliminarily graded using the AREDS classification system.[28] Patients with non-neovascular AMD and at least one large druse (≥125 μm) and no signs of geographic atrophy at the foveal center were recruited (Figs. 1A, 1B). This is considered intermediate AMD and corresponds to AREDS level 3.[28] Included were 63 eyes of 41 patients (aged 53–83 years). Best-corrected visual acuities ranged from 20/20 to 20/50; 56 of 63 eyes had 20/25 or better visual acuity while the remaining seven were in the range of 20/32 to 20/50. Spherical equivalent refractive errors ranged from −3.25 to +4.00 diopters (D). A control group of older Amish subjects with normal eye examinations ($n = 10$; aged 51–79 years) were used to determine retinal structural parameters in healthy eyes for comparison with the AMD eyes. Best-corrected visual acuities were all 20/20. Spherical equivalent refractive errors ranged from −1.75 to +1.50 D. For all subjects, ocular and medical histories were obtained and a routine eye examination was performed. Institutional review board approval and informed consent were obtained, and the procedures adhered to the tenets of the Declaration of Helsinki.

Imaging and Analyses

OCT was performed with a spectral-domain (SD) system (RTVue-100; Optovue, Inc., Fremont, CA). Cross-sectional imaging included a protocol with 4.5- or 9-mm line scans along the horizontal and vertical meridia crossing the fovea, and 6 × 6 mm raster scans (101 lines with 513 longitudinal reflectivity profiles [LRPs] each) centered at the fovea providing high density coverage of the macula. En face imaging was performed with a confocal scanning laser ophthalmoscope (Spectralis HRA; Heidelberg Engineering GmbH, Heidelberg, Germany). Retinal and subretinal features were imaged with near-infrared reflectance under high-speed mode and with frame averaging using automatic-real-time feature of the manufacturer.

In AMD patients, an OCT en face projection image[17] was produced by the manufacturer's software (RTVue-100 version 6.1.0.4; Optovue, Inc.) by integrating the backscatter intensity along a ~20-μm slice parallel to BrM to produce a bright background image with darker regions corresponding to drusen (Fig. 1C). Eyes with one or more large (≥125 μm) drusen visible on the OCT en face image were analyzed further. For each large druse, the retinal location of the peak drusen height and a neighboring paradrusen location with no apparent RPE elevation were recorded with respect to the location of the fovea. For subfoveal drusen, only the peak location was defined without a paradrusen location.

Segmentation of the retinal layers was performed manually (Fig. 1D). The hyposcattering ONL layer was defined between the hyperscattering outer plexiform layer (OPL) and the hyperscattering outer limiting membrane (OLM). The OPL/ONL boundary was chosen on the scleral transition of the most vitreal OPL peak visible near the hyposcattering inner nuclear layer (INL). The layers encompassing the inner and outer segments (IS+OS) of photoreceptors were defined manually between OLM and the hyperscattering peak near the interface of rod OS tips and apical RPE processes.[29] Drusen, when present, were defined between the RPE and BrM (Fig. 1D). For each druse, maximum width and maximum height were measured. At the retinal location of peak drusen height and a paired paradruse location, ONL and IS+OS thickness were measured (Fig. 1D). In a subset of AMD eyes (32 eyes of 24 AMD patients), ONL and IS+OS thickness were measured at 16 fixed locations distributed along the four boundaries of the 6 × 6 mm raster scans in order to obtain estimates of photoreceptor parameters as distant as possible from the drusen, which tended to be located in the parafoveal region.

A broad hyperscattering region originating from the Henle fiber layer (HFL) can appear scleral to the OPL. The visibility of the HFL layer can change due to local abnormalities, such as drusen, which affect the paths of incident and backscattered rays.[30] Our choice of OPL/ONL boundary is vitreal to the HFL reflection and thus, our definition of ONL thickness reported herein is expected to include the anatomical layers of both ONL and HFL.[31] To evaluate a potential underestimation of the ONL thickness above drusen with variable HFL layer visibility, 143 drusen in a subset of eyes (12 eyes of 12 AMD patients) were evaluated with a semiautomated technique based on the detection of the inner plexiform layer (IPL) and results compared with the manual segmentation based on the detection of the OPL (Fig. 1E). For this purpose, the manufacturer's automated algorithm (Optovue, Inc.) was used. The difference between paradrusen and peak drusen thicknesses measured with the semiautomated method was compared to the differences measured at the same pairs of loci with the manual method. The relationship between the two methods was fit with a linear regression line of near unity slope and near zero intercept (Fig. 1E). Assuming the underlying physiological distance from OPL to INL/IPL boundary is similar at neighboring pairs of loci, this comparison implies a lack of bias in manually placing the vitreal ONL boundary at drusen loci with variably visible HFL signal.

In the older normal subjects, ONL and IS+OS thicknesses were measured on a square grid with 0.5-mm sampling in the 2 × 2 mm region centered at fovea, and with a 1-mm sampling across the rest of the 6 × 6 mm raster scan. The summary statistics (mean and ±2 SD) were formed on a 0.5-mm grid interpolated as necessary by bilinear interpolation. ONL and IS+OS measures of AMD eyes were specified as "fraction" of the respective mean normal value corresponding to the retinal location. In a subset of AMD eyes, more complex OCT data analyses were performed using custom programs (MATLAB 7.5; MathWorks, Natick, MA); the results were quantitatively compared with OCT data from aged normals ($n = 10$) processed with the same methods. In these subanalyses, vertical line scans (23 eyes of 19 AMD patients) or central macular raster scans (6 eyes of 6 AMD patients) were segmented using intensity and local slope of LRPs with methods previously published.[32–34] ONL measurements were compared with normal limits (mean ±2 SD) and locations showing significant changes were marked. Locations of the drusen with substantial elevations of the RPE above BrM were outlined.

RESULTS

Reductions in Photoreceptor Layer Thickness Are Related to Drusen Size

In our group of older normal Amish subjects' eyes, both ONL and IS+OS are at maximal thickness at the fovea and decrease with increasing eccentricity across the macula (Fig. 2A). The foveal ONL thickness was 111.3 ± 10.5 μm (mean ± SD) consistent with published measures in normal eyes,[35–41] which tend to show thickening with normal aging.[31,35,40–42] At 3-mm eccentricity, ONL thickness was 62.3 ± 4.9, 56.3 ± 3.6, 57.4 ± 4.6, and 58.1 ± 4.5 μm along the superior, inferior, temporal, and nasal retinal meridians, respectively. The IS+OS thickness at the fovea was 81.4 ± 3.1 μm; and at 3-mm eccentricity, it was 54.0 ± 3.2, 50.9 ± 2.2, 51.0 ± 1.7, and 52.1 ± 3.1 μm along superior, inferior, temporal, and nasal retinal meridians, respectively.

In the maculae of the AMD patients, the spatial distribution of the 750 large drusen that we analyzed is displayed on an en face image (Fig. 2B). The majority of these drusen (442/750; 59%) were concentrated in the foveal and parafoveal region extending to 1.5-mm eccentricity. The distribution of drusen was circularly isotropic and did not favor any specific retinal quadrant. Average width of the drusen was 352 (±153) μm and the average height was 78 (±31) μm.

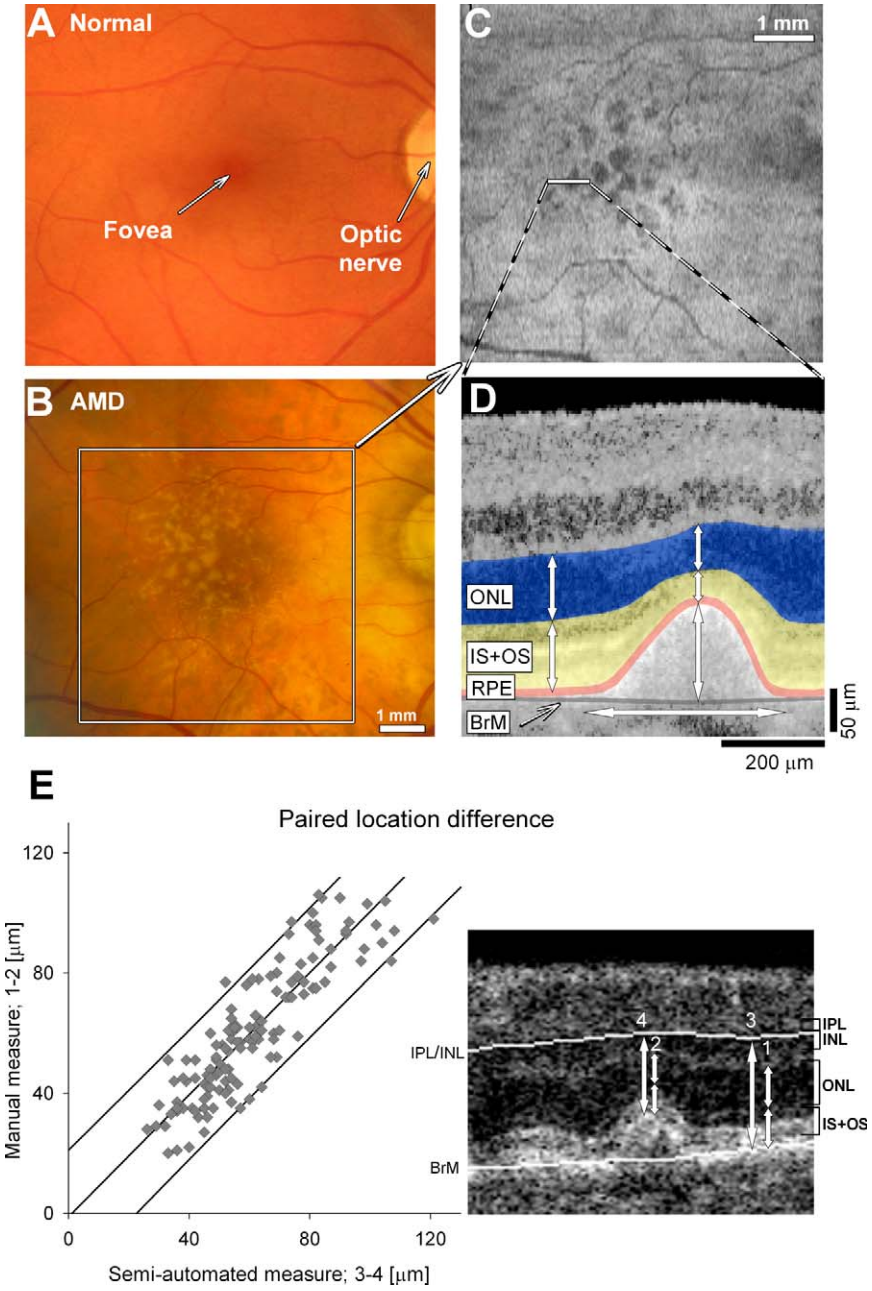

Figure 1. Quantitation of the photoreceptor layer in intermediate AMD eyes at and near large drusen. **(A, B)** Color fundus photograph in an older normal subject **(A)** and in a patient with intermediate AMD and drusen **(B)**. *Square region* in **(B)** shows the location of the central macular 6×6 mm OCT raster scan performed. **(C)** En face OCT projection image showing the integrated intraretinal backscatter intensity along a ~20-µm slice parallel to BrM. Darker regions correspond to drusen that were analyzed further if they were ≥125 µm. **(D)** Enlarged OCT scan displaying large drusen microstructure. Layers highlighted for visibility: ONL in *blue*, IS+OS in *yellow*, RPE in *orange*, and BrM as a *dark gray line*. Dome-like separation of the RPE from BrM shows a large druse. *Arrows* depict the ONL and IS+OS measures at the peak of the druse and at a neighboring paradruse locus. Drusen height at peak and horizontal width at the base are also marked with *arrows*. **(E)** Comparison of the manual measurement procedure with a semiautomated procedure (in 12 eyes of 12 AMD patients; 143 pairs of drusen and paradrusen loci). This comparison was performed to understand whether a bias is introduced into manual segmentation of the vitreal ONL boundary by variable intrusion of HFL intensity at peak drusen and paradrusen locations. Plot shows no evidence of bias with the correlation line having a near unity slope and near zero intercept. *Inset: Arrows 1 and 2* show the manual measurement of ONL+IS+OS at paradruse and peak druse locations, respectively. *Arrow 3* is the thickness measured from an automated boundary (between the inner plexiform layer, IPL and inner nuclear layer, INL) to another automated boundary (BrM) at a paradrusen locus. *Arrow 4* is the thickness measured from the automated boundary (IPL/INL) to the bright RPE signal at the peak of drusen (automated segmentation of the RPE layer was not reliable under drusen). If there is an artefactual reduction of ONL above drusen due to variable involvement of the HFL, ONL+IS+OS loss implied by the manually-determined difference 1-2 would be expected to be larger than the loss implied by the semi-automatically–determined difference 3-4.

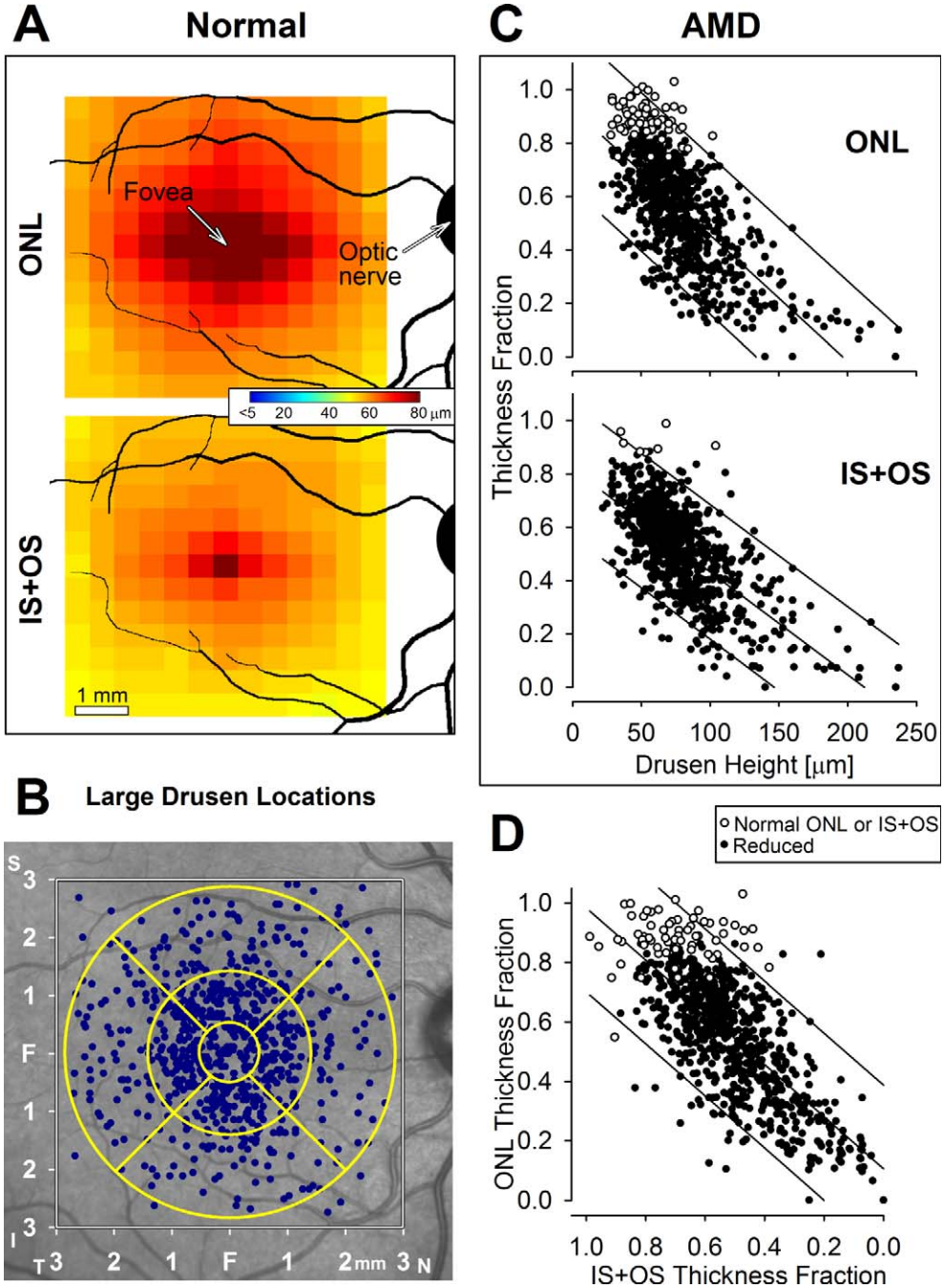

Figure 2. Photoreceptor parameters in normal and AMD eyes. (**A**) Spatial distribution of the mean ONL and IS+OS thickness in older normal subjects, displayed on a pseudocolor scale across a 0.5-mm square grid centered at the fovea of a right eye. Schematic representation of the location of the major blood vessels and optic nerve is shown. Pseudocolor scale is between the maps. (**B**) Spatial distribution of all large drusen analyzed ($n = 750$) from all AMD patients in right-eye equivalent representation (*filled blue circles*). In the background is a near-infrared reflectance image for orientation. The 6×6 mm area where measurements were made (*square*) and the standard Early Treatment of Diabetic Retinopathy Study (ETDRS) grid (*yellow circles*) are displayed. (**C**) ONL (*upper*) and IS+OS (*lower*) thickness fractions measured above drusen as a function of the maximum height of drusen. *Open circles* represent results within normal limits, and *filled black circles* are those with significant reduction. (**D**) Relationship between ONL and IS+OS thickness above drusen. *Open circles* represent results within normal limits for ONL or IS+OS measures. In (**C**, **D**), lines through data indicate linear regression and 95% prediction intervals.

The photoreceptor laminae overlying the drusen were abnormal. ONL thickness measured at the peak height of each druse was compared with location-matched control values, and 689/750 loci (92%) showed significant (>2 SD) thinning. On average, the reduction in overlying ONL thickness was 48% of the mean normal value. The extent of ONL thickness reduction was strongly related to maximum drusen height (Fig. 2C, upper panel; $r^2 = 0.48$, 46% decrease in ONL per 100-µm increase in drusen height).

To investigate further the effects of drusen on outer retinal architecture, we asked whether the reductions in ONL over drusen were accompanied by changes in the photoreceptor

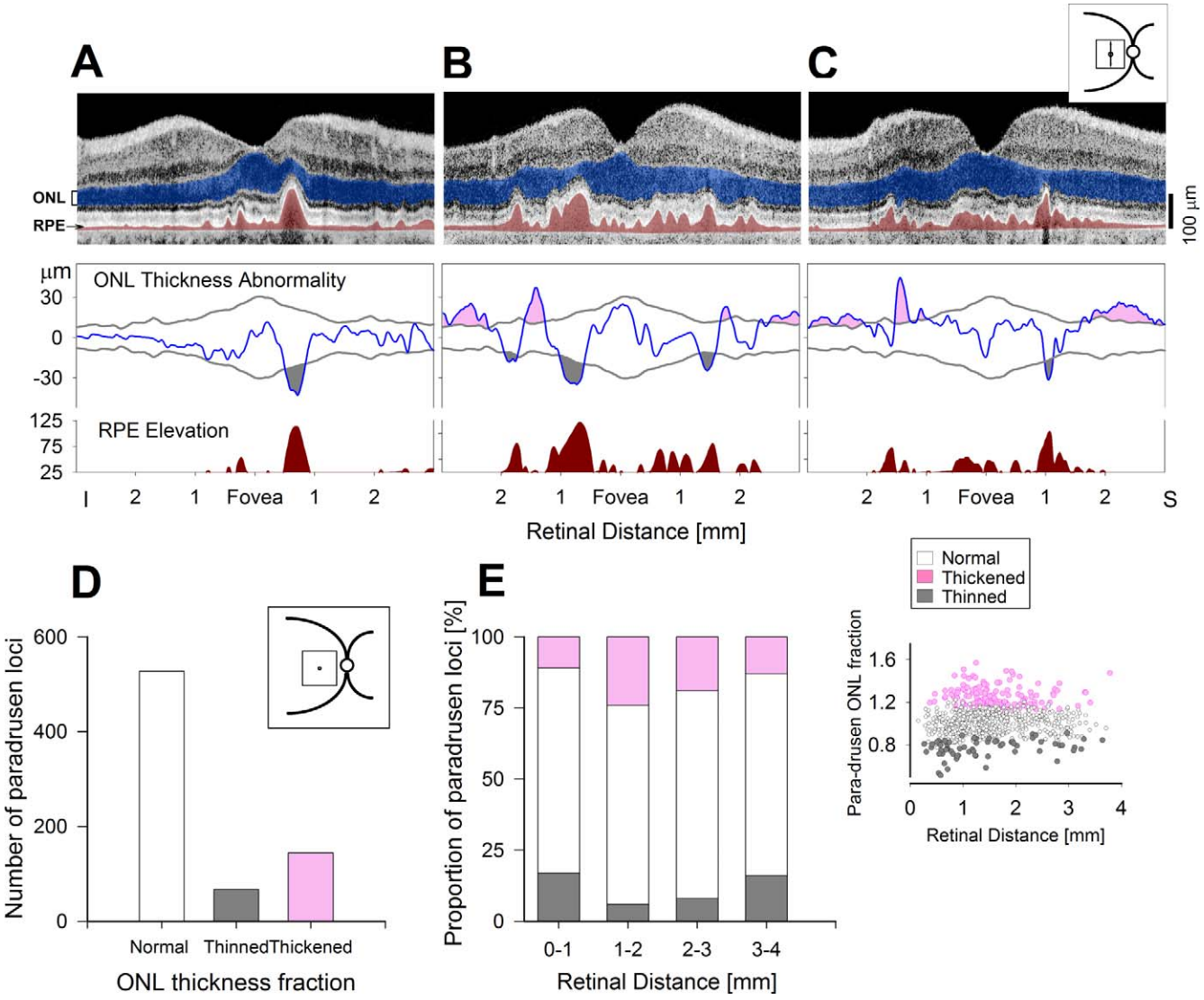

Figure 3. Changes in ONL thickness in paradrusen regions of AMD eyes. (**A–C**) *Upper panels* depict vertical scans through the fovea in the central 6 mm of retina in three AMD patients representing different ONL thickness changes. ONL is highlighted *blue* and the region between the RPE and BrM is highlighted *deep red*. *Middle panels* show the ONL thickness difference between each AMD patient and a group of normal elderly subjects ($n = 10$; limits of normal mean shown with *gray lines*, ±2 SD). *Lower panels* show drusen corresponding to the RPE elevations rising above 25 µm. (**A**) AMD patient with only a single locus with ONL reduction (colored *gray*) and this is above a druse. Paradrusen region is devoid of abnormalities in ONL thickness. (**B**, **C**) Two AMD patients with ONL reductions (*gray*) associated with drusen, and ONL increases (*pink*) in paradrusen areas. *Inset*: location of the 6-mm vertical scan on a schematic of the fundus. (**D**) Histograms of the number of paradrusen loci with ONL thickness that are within normal limits ($n = 527$); reduced ($n = 67$); and increased ($n = 144$). *Inset*: schematic representation of the 6×6 mm macular region sampled. (**E**) *Bar graphs* representing the proportion of the three categories of paradrusen ONL thickness as a function of retinal distance from the fovea. Normal is shown as *white*, abnormally reduced thickness as *gray*, and abnormally increased thickness as *pink*. There is no obvious pattern of distribution to the abnormal paradrusen ONL loci. *Inset*, *right*: shows paradrusen ONL fraction of mean normal thickness as a function of eccentricity.

IS+OS layer. The IS+OS layer thickness overlying drusen was also reduced and strongly related to drusen height (Fig. 2C, lower panel; $r^2 = 0.46$, 38% decrease in IS+OS per 100-µm increase in drusen height). The thickness fractions of ONL and IS+OS overlying drusen were correlated ($r^2 = 0.53$) with a linear regression slope of near unity (Fig. 2D). The great majority of loci (685/750; 91%) showed abnormally reduced ONL and IS+OS thickness. Among the rest of the loci, 58/750 (~8%) showed normal ONL, but reduced IS+OS; four loci had reduced ONL and normal IS+OS, and three loci had both normal ONL and IS+OS thickness. These cross-sectional results suggested that IS+OS disease may precede ONL thinning.

Paradrusen Retinal Regions Can Show Photoreceptor ONL Layer Thickening

ONL thickness was also measured in regions neighboring drusen to determine whether abnormally reduced photoreceptor laminae were also present in these paradrusen regions without RPE elevation. We first performed an observational study of outer retinal architecture with line scans along the

vertical meridian extending 3 mm superior and 3 mm inferior to the fovea in 23 eyes of 19 AMD patients. Of the 23 eyes, 18 had drusen greater than 50 μm in height and served to confirm the observations from the raster scans that ONL thickness was reduced in association with taller drusen, as illustrated by the results in an AMD patient (Fig. 3A; gray highlights). Paradrusen loci in seven of the 18 eyes showed ONL thickness that was within normal limits (not shown). Eleven of the 18 eyes had the surprising finding of increased thickening of the ONL at paradrusen regions (Figs. 3B, 3C; pink highlights). Five of 23 eyes had no drusen that were greater than 50 μm in height. ONL thickness above these smaller drusen (or edges of larger drusen not captured in the scan) was within normal limits (not shown). Paradrusen loci were also within normal limits for ONL thickness, for the most part, with the exception of two eyes that showed one or several regions with abnormally thickened ONL compared with the limits (mean +2 SD) in aged normal eyes.

The surprising observation of thickened ONL on the vertical profiles through the central retinas of AMD patients prompted us to extend our analyses away from the midline to raster scans covering the macula in two dimensions. We quantified photoreceptor thickness at paradrusen areas (738 loci) that were qualitatively selected to have normal-appearing laminar architecture without RPE elevation as close as possible to previously identified drusen in 63 AMD eyes. ONL and IS+OS measurements at paradrusen locations mimicked the analyses we had performed over drusen (Fig. 2). Nearly three-fourths of paradrusen loci (527/738; 71.5%) showed ONL that was within the normal limits. Some of these paradrusen areas, however, showed substantial thinning of the ONL (67/738 locations; 9%) when compared with location-matched normal limits (Fig. 3D). Further, we found paradrusen areas that had significant thickening of the ONL (144/738 locations; 19.5%) when compared with location-matched normal limits (Fig. 3D). The latter measurements confirmed and extended the observations in the vertical profiles.

There was no spatial pattern of distribution for these paradrusen changes in ONL. Paradrusen locations with thickened ONL, normal ONL, as well as locations with decreased ONL were found at all eccentricities measured (Fig. 3E). The distance between paradrusen locations with thickened ONL and the locus of peak height of their neighboring drusen (311 ± 135 μm) was not different than the distance at normal (302 ± 119 μm) or thinned (313 ± 188 μm) paradrusen locations. There were no obvious clinical features that distinguished eyes ($n = 38$) with evidence of thickened ONL loci from the entire cohort of intermediate AMD eyes we analyzed: 18% of the eyes with thickened ONL versus 16% of all AMD eyes had intraocular lenses; median spherical equivalent refraction (in the subset of patients with natural lenses) was 0.25 D in eyes with thickened ONL versus plano in all intermediate AMD eyes (range was identical: −3.25 to +4.00 D); and median age and range of ages was identical (median 74 years, range 53–83 years) in eyes with thickened ONL versus in all eyes.

Macular Topography Shows ONL Thickening Distant to Drusen

To understand whether ONL thickening was only associated with paradrusen regions or if it could also be observed distant to drusen, we quantified photoreceptor parameters in a subset of 32 AMD eyes at the boundaries of the 6 × 6 mm macular raster scans where drusen were more rarely found (Fig. 2B). Specifically, 16 loci (at eccentricities of 3–4.24 mm) were sampled in each eye and compared with normal limits. Nine of 32 eyes (28%) showed one or more loci with abnormally thickened ONL at these pericentral locations. For a subset of four AMD patients with pericentral ONL thickening and two patients without such evidence, high-resolution maps of ONL topography and thickness differences from normal controls were generated to better understand the spatial extent of the regions both near and distant to drusen that showed changes in ONL thickness. Results from these six AMD patients (Fig. 4) were as follows: A 78-year-old patient with 13 large drusen peaks (average elevation, 85 μm) distributed in the parafoveal region showed delimited regions of paradrusen ONL thickening (Fig. 4A). Maximum ONL thickening was 7.5 μm above normal limits. Most of the paradrusen regions and all of the perifoveal region distant from drusen had ONL thickness within normal limits. A 76-year-old patient also with 13 large drusen peaks (average elevation, 113 μm) in the parafoveal region showed ONL thickening at the foveal region as well as many paradrusen regions (Fig. 4B). Maximum ONL thickening was 34 μm above normal limits. A 79-year-old patient with 23 large drusen peaks (average elevation, 79 μm) in the perifoveal region showed ONL thickening in paradrusen regions as well as in regions more distant to drusen (Fig. 4C). Maximum ONL thickening was 16 μm above normal limits. An 82-year-old patient with 19 large drusen peaks (average elevation, 70 μm) in the para- and perifoveal regions showed some paradrusen thickening as well as thickening distant to drusen (Fig. 4D). Maximum ONL thickening was 12 μm above normal limits. A 74-year old patient with seven perifoveal drusen (average elevation, 72 μm; Fig. 4E) and an 81-year-old patient with 17 para- and perifoveal drusen (average elevation, 89 μm; Fig. 4F) showed extensive regions of ONL thickening distant from drusen. Maximum ONL thickenings were 16 and 20 μm above normal limits, respectively. These examples in a subset of intermediate AMD eyes demonstrate that ONL thickening is detectable in the immediate vicinity of large drusen as well as distant to drusen.

Discussion

Photoreceptor Layers Overlying Drusen Are Abnormally Reduced

In vivo cross-sectional imaging of the retina with OCT allows quantitation of photoreceptor laminae in the living eye and has become an important tool for investigating and understanding retinal diseases. Our results of quantifying photoreceptor structure by OCT in a cohort of Caucasian AMD patients of Amish origin confirm and extend previous findings in other populations (e.g., see Refs. 19 and 21). There was a linear relationship between photoreceptor laminar decrease and drusen height. Recognizing that OS shortening is an early feature of hereditary retinal degenerations,[43] we determined the relationships with drusen of the IS+OS and ONL laminae separately. The IS+OS layer was reduced over drusen, as has been previously reported.[21] Of interest, a minority (~8%) of loci showed reduced IS+OS but normal thickness of ONL, possibly indicating a disease sequence although serial data will be required to clarify this.[21] Reductions in IS+OS were directly proportional to reductions in ONL, a finding consistent with results in animal models of retinal degeneration in which there have been demonstrations of proportional rod outer segment shortening and ONL loss by histopathology.[44] We acknowledge that our ONL thickness measures included the HFL layer, the visibility of which may be complicated by the imaging geometry and distorting effects of protruding drusen, and lead to overestimation of ONL reductions.[30] In the current study, this potential artifact

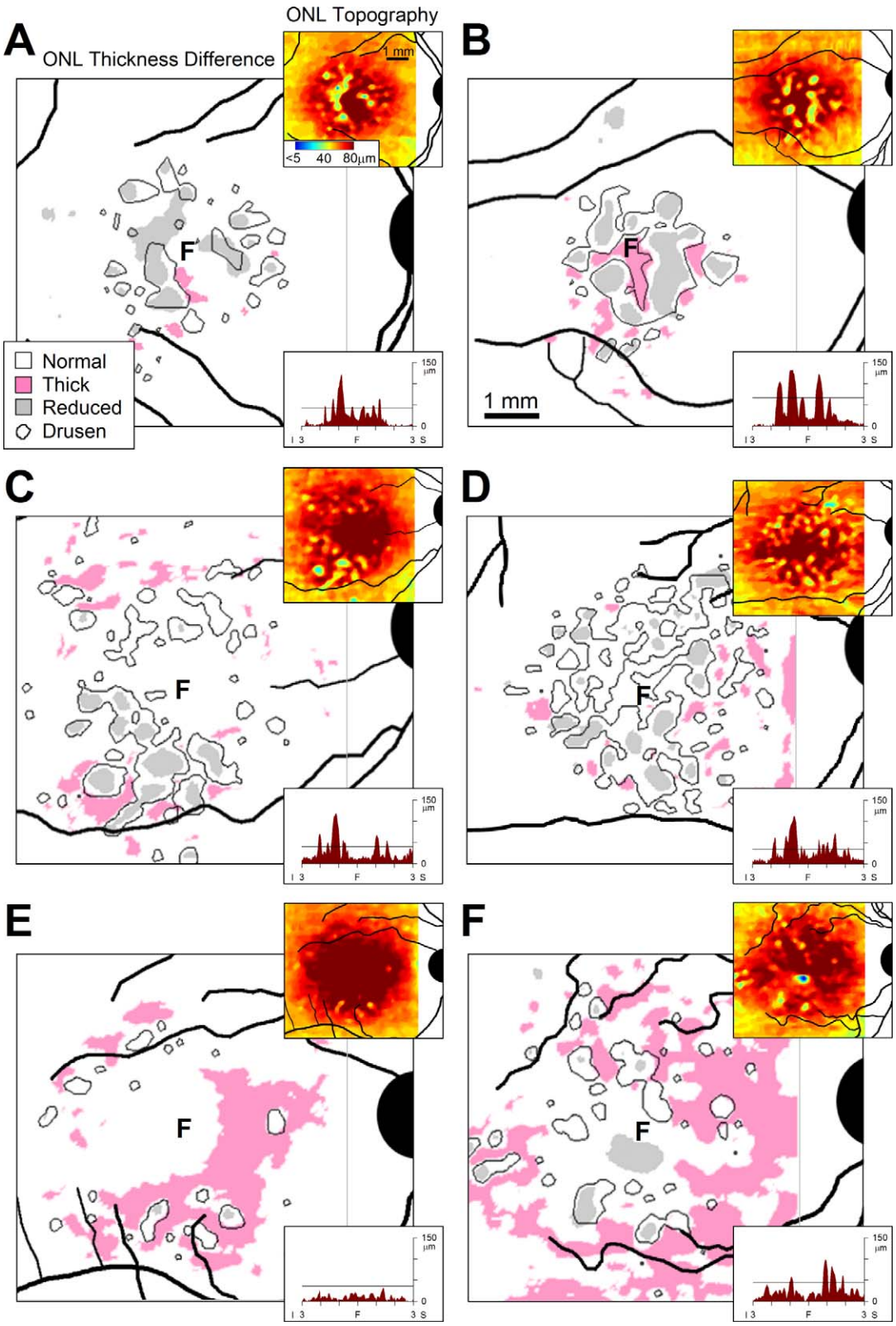

Figure 4. Spatial topography of the photoreceptor ONL thickness and drusen across maculae of AMD patients. (**A–F**) Differences in ONL thickness between intermediate AMD patients and a group of age-matched normal subjects. The magnitude of the differences are categorized into three types: locations that are within 2 SD of normal variation (*white*); significantly reduced in thickness (*gray*, <2 SD from mean normal at each locus); and significantly increased in thickness (*pink*, >2 SD). Substantial RPE elevations are outlined (*black irregular lines*) at 50% of average height for the analyzed large drusen in each eye. Schematics of retinal vessels and optic nerve head are overlaid; all maps are shown as right eyes for comparability. F, fovea. *Insets*, *upper right*: show pseudocolor maps of ONL thickness in AMD patients sampled at high resolution across a 6 × 6 mm region centered at the fovea. *Insets*, *lower right*: show RPE elevation along the vertical meridian crossing the fovea. *Black lines* indicate the cutoff (50% of average height) used for outlining drusen boundaries.

was addressed through multiple methods of measuring the outer retinal thickness to confirm the results presented.

Relationship of In Vivo Imaging Results to Histopathologic Studies in AMD

What do our OCT results of ONL and IS+OS reduction above drusen mean? Histopathological studies of postmortem eye donor tissue indicate varying degrees of photoreceptor cell loss overlying drusen.[15,45–47] Rod and cone IS and OS have been shown to be distorted by the protruding drusen and OS are shortened. As we found noninvasively, the abnormalities in photoreceptor IS and OS in donor retinas have been reported to be related to drusen size, both height and width.[46] What is not known is whether our findings at a single timepoint showing reduced photoreceptor parameters are indeed the in vivo correlates of the single timepoint histopathology that shows similar results. There is a temptation to relate the two data sets, but the literature on AMD pathogenesis and progression suggests that the connection may not be so simple. Regression of drusen is known to occur from en face fundus studies (e.g., see Refs. 48–50) and has been documented by OCT.[51] Although not specifically addressed or measured, some published images of serial OCTs in AMD show that ONL, which is reduced overlying drusen at one timepoint, may increase to more normal-appearing thickness at a later time (e.g., see Figs. 3 and 5 in Yehoshua et al.[51]). Obviously needed are further longitudinal OCT data measuring photoreceptor parameters as well as drusen parameters. There is no doubt that photoreceptor degeneration occurs in AMD and that drusen are harbingers of the disease, but the exact disease sequence requires clarification so that clinical trial results are not misinterpreted when a treatment is associated with OCT change that may simply be part of the natural history.

How can a dynamic ONL reduction with reversal be explained? Among the proposed pathogenic processes resulting from protruding drusen is physical displacement of ONL and IS+OS.[46] This is unlikely to be without later consequence and may be one of many components of cumulative photoreceptor stress. Other suspected mechanisms for photoreceptor degeneration beyond the compressing effects of drusen include drusen-induced impairment of metabolic exchange from RPE and choroid, and activation of the immune system with negative sequelae.[6,7,46,52]

Regions Neighboring Drusen Can Have Increased Thickness of the ONL

The ONL measurements in paradrusen locations indicated that most fell within the normal limits of locus-specific older control data. Other regions adjacent to large drusen had significantly reduced ONL thickness. Why would there be thinned ONL in areas with no overlying drusen? One explanation is that a diffuse degenerative process ensues in AMD and results in photoreceptor losses regardless of its relationship to drusen. Histopathological studies (e.g., see Ref. 15) have shown that widespread photoreceptor loss can be present in AMD. Alternatively, regressing drusen can lead to degeneration of the RPE and photoreceptor layer and result in geographic atrophy. Drusen have a dynamic nature and can spontaneously shrink or regress at times.[49,50] Focal patches of atrophy left by the fading of most drusen, as well as generalized drusen related atrophy, have been described.[14]

An unexpected finding was that there were regions of ONL thickening neighboring large drusen. With topographic mapping in a subset of patients, the thickening was not limited to paradrusen loci in the central macula, but could also be found near the peripheral edges of the macula distant from drusen. The magnitude of thickening we measured in intermediate AMD patients could extend 8 to 34 μm beyond the age- and race-matched normal limits. Our results suggest that the photoreceptor disease in AMD is more complex than a localized loss of photoreceptors due to drusen. Several hypotheses could explain the finding of thickened ONL. One possibility is that chronic degenerative stress is causing hypertrophy of Müller cell processes that extend through the ONL and cause thickening, before overt atrophy ensues. A basal level of photoreceptor stress may exist with normal aging, which has been speculated to contribute to the thickening of the foveal ONL observed with age.[31,35,40–42] It is of interest that in late stage AMD with geographic atrophy and foveal sparing, there can be thickening of the residual foveal ONL; this has been postulated to result from a preapoptotic stage.[53] In other retinal degenerative conditions, such as retinitis pigmentosa (RP), one of the earliest disease features that appear before degeneration is Müller cell hypertrophy in stressed retina.[25] Local injury, in the form of cell loss, has been shown to provoke a Müller cell reaction as a response to neuronal insult. Müller glial reaction after laser photocoagulation in the mouse retina, for example, has been demonstrated.[54] Laser injury stimulated local Müller cell activation and directed migration of nuclei into the ONL. This type of Müller cell migration could potentially contribute to the ONL thickening that we observed. Paradrusen regions with photoreceptor layer thickening may be caused by degenerative stress, which has been suggested to represent the earliest signs of photoreceptor loss, and a phase that precedes degeneration. Several studies have observed increases in photoreceptor layers in retinal degenerative diseases.[23,24,26] Retinas of carriers of canine models of *RPGR*-XLRP have patchy degeneration with an increased ONL thickness corresponding to areas of diseased rods in early disease stages. In later stages, these regions developed a generalized thinning of the ONL. Some of the patients we studied with *NPHP5*- and *NPHP6*-LCA had regions with increased ONL thickness.[26] These regions were in rod-dominant areas and were postulated to be early signs of retinal stress.[26]

Alternatively, photoreceptor stress and cell loss can result in increased levels of growth factors, leading to thickening of the ONL surrounding the drusen. Growth factors are naturally released upon photoreceptor injury such as mechanical, laser, or light damage, and many studies have suggested that retinal insult can result in a photoreceptor protective effect (e.g., see Refs. 55–58). In one study, local photoreceptor rescue extended to a 250-μm area surrounding needle injury in the Royal College of Surgeons' rat model of retinal degeneration,[55] while another study used a light damage model of retinal degeneration and showed local photoreceptor rescue after needle insult with the effect extending from 100 to 800 μm.[56] Human retinas showed localized neurotrophins in regions adjacent to long-term (5–12 years) laser scars.[58] In the current study, the average distance between loci with thickened ONL and the center of neighboring large drusen was 311 μm. This distance would be consistent with the local range of growth factor increases under different experimental paradigms mentioned above, and would fit with a hypothesis of regional growth factors responding to cell death above drusen. Moreover, when considering the average width of the drusen neighboring these thickened loci, the distance to the edge of the drusen would be even less, and <200 μm, on average. Finally, the wealth of new information about activation of the immune system and the evidence for a role of inflammation in early AMD prompts the question of how this may relate to our finding of thickened ONL in the current study. The exact sequence from activated inflammasome to the photoreceptor layer effects we observed is not known but worth exploring in

detail, especially if the photoreceptor effects are markers for early disease in retina away from drusen.[52,59] Our findings can also yield insight into why studies measuring localized function in retinal regions with drusen have not yielded results with a clear consensus (e.g., see Refs. 60–63). Some studies found a similar sensitivity loss in drusen versus nondrusen areas; others found lower sensitivities in drusen versus nondrusen areas; and others found decreased sensitivity in some drusen areas (compared with nondrusen areas) but not in others. Our in vivo anatomical findings of normal, decreased, and increased photoreceptor layer thickness in areas next to drusen suggest that the structure-function relationship could be more complex than previously considered.

References

1. Rattner A, Nathans J. Macular degeneration: recent advances and therapeutic opportunities. *Nat Rev Neurosci*. 2006;7:860–872.
2. Jager RD, Mieler WF, Miller JW. Age-related macular degeneration. *N Engl J Med*. 2008;358:2606–2617.
3. Coleman HR, Chan CC, Ferris FL III, Chew EY. Age-related macular degeneration. *Lancet*. 2008;372:1835–1845.
4. Hageman GS, Luthert PJ, Victor Chong NH, Johnson LV, Anderson DH, Mullins RF. An integrated hypothesis that considers drusen as biomarkers of immune-mediated processes at the RPE-Bruch's membrane interface in aging and age-related macular degeneration. *Prog Retin Eye Res*. 2001;20:705–732.
5. Swaroop A, Chew EY, Rickman CB, Abecasis GR. Unraveling a multifactorial late-onset disease: from genetic susceptibility to disease mechanisms for age-related macular degeneration. *Annu Rev Genomics Hum Genet*. 2009;10:19–43.
6. Gu J, Pauer GJ, Yue X, et al. Assessing susceptibility to age-related macular degeneration with proteomic and genomic biomarkers. *Mol Cell Proteomics*. 2009;8:1338–1349.
7. Yu Y, Reynolds R, Rosner B, Daly MJ, Seddon JM. Prospective assessment of genetic effects on progression to different stages of age-related macular degeneration using multistate Markov models. *Invest Ophthalmol Vis Sci*. 2012;53:1548–1556.
8. Gorin MB. Genetic insights into age-related macular degeneration: Controversies addressing risk, causality, and therapeutics. *Mol Aspects Med*. 2012;33:467–486.
9. Veritti D, Sarao V, Lanzetta P. Neovascular age-related macular degeneration. *Ophthalmologica*. 2012;227;11–20.
10. Gehrs KM, Anderson DH, Johnson LV, Hageman GS. Age-related macular degeneration–emerging pathogenetic and therapeutic concepts. *Ann Med*. 2006;38:450–471.
11. Sallo FB, Peto T, Leung I, Xing W, Bunce C, Bird AC. The International Classification system and the progression of age-related macular degeneration. *Curr Eye Res*. 2009;34:238–240.
12. Chong EW, Wong TY, Kreis AJ, Simpson JA, Guymer RH. Dietary antioxidants and primary prevention of age related macular degeneration: systematic review and meta-analysis. *BMJ*. 2007;335:755.
13. Green WR, Key SN III. Senile macular degeneration: a histopathologic study. *Trans Am Ophthalmol Soc*. 1977;75:180–254.
14. Sarks JP, Sarks SH, Killingsworth MC. Evolution of geographic atrophy of the retinal pigment epithelium. *Eye (Lond)*. 1988;2:552–577.
15. Curcio CA, Medeiros NE, Millican CL. Photoreceptor loss in age-related macular degeneration. *Invest Ophthalmol Vis Sci*. 1996;37:1236–1249.
16. Khanifar AA, Koreishi AF, Izatt JA, Toth CA. Drusen ultrastructure imaging with spectral domain optical coherence tomography in age-related macular degeneration. *Ophthalmology*. 2008;115:1883–1890.
17. Gorczynska I, Srinivasan VJ, Vuong LN, et al. Projection OCT fundus imaging for visualising outer retinal pathology in non-exudative age-related macular degeneration. *Br J Ophthalmol*. 2009;93:603–609.
18. Leuschen JN, Schuman SG, Winter KP, et al. Spectral-domain optical coherence tomography characteristics of intermediate age-related macular degeneration. *Ophthalmology*. 2013;120:140–150.
19. Schuman SG, Koreishi AF, Farsiu S, Jung SH, Izatt JA, Toth CA. Photoreceptor layer thinning over drusen in eyes with age-related macular degeneration imaged in vivo with spectral-domain optical coherence tomography. *Ophthalmology*. 2009;116:488–496.
20. Godara P, Siebe C, Rha J, Michaelides M, Carroll J. Assessing the photoreceptor mosaic over drusen using adaptive optics and SD-OCT. *Ophthalmic Surg Lasers Imaging*. 2010;41;S104–S108.
21. Hartmann KI, Gomez ML, Bartsch DU, Schuster AK, Freeman WR. Effect of change in drusen evolution on photoreceptor inner segment/outer segment junction. *Retina*. 2012;32:1492–1499.
22. Jacobson SG, Cideciyan AV, Aleman TS, et al. Crumbs homolog 1 (CRB1) mutations result in a thick human retina with abnormal lamination. *Hum Mol Genet*. 2003;12:1073–1078.
23. Beltran WA, Wen R, Acland GM, Aguirre GD. Intravitreal injection of ciliary neurotrophic factor (CNTF) causes peripheral remodeling and does not prevent photoreceptor loss in canine RPGR mutant retina. *Exp Eye Res*. 2007;84:753–771.
24. Beltran WA, Acland GM, Aguirre GD. Age-dependent disease expression determines remodeling of the retinal mosaic in carriers of RPGR exon ORF15 mutations. *Invest Ophthalmol Vis Sci*. 2009;50:3985–3995.
25. Jacobson SG, Cideciyan AV. Treatment possibilities for retinitis pigmentosa. *N Engl J Med*. 2010;363:1669–1671.
26. Cideciyan AV, Rachel RA, Aleman TS, et al. Cone photoreceptors are the main targets for gene therapy of NPHP5 (IQCB1) or NPHP6 (CEP290) blindness: generation of an all-cone Nphp6 hypomorph mouse that mimics the human retinal ciliopathy. *Hum Mol Genet*. 2011;20:1411–1423.
27. Peet JA, Cotch MF, Wojciechowski R, Bailey-Wilson JE, Stambolian D. Heritability and familial aggregation of refractive error in the Old Order Amish. *Invest Ophthalmol Vis Sci*. 2007;48:4002–4006.
28. Age-Related Eye Disease Study Research Group. The Age-Related Eye Disease Study system for classifying age-related macular degeneration from stereoscopic color fundus photographs: AREDS report No. 6. *Am J Ophthalmol*. 2001;132:668–681.
29. Spaide RF, Curcio CA. Anatomical correlates to the bands seen in the outer retina by optical coherence tomography: literature review and model. *Retina*. 2011;31:1609–1619.
30. Lujan BJ, Roorda A, Knighton RW, Carroll J. Revealing Henle's fiber layer using spectral domain optical coherence tomography. *Invest Ophthalmol Vis Sci*. 2011;52:1486–1492.
31. Curcio CA, Messinger JD, Sloan KR, Mitra A, McGwin G, Spaide RF. Human chorioretinal layer thicknesses measured in macula-wide, high-resolution histologic sections. *Invest Ophthalmol Vis Sci*. 2011;52:3943–3954.
32. Huang Y, Cideciyan AV, Papastergiou GI, et al. Relation of optical coherence tomography to microanatomy in normal and rd chickens. *Invest Ophthalmol Vis Sci*. 1998;39:2405–2416.
33. Jacobson SG, Cideciyan AV, Gibbs D, et al. Retinal disease course in Usher syndrome 1B due to MYO7A mutations. *Invest Ophthalmol Vis Sci*. 2011;52:7924–7936.

34. Jacobson SG, Cideciyan AV, Peshenko IV, et al. Determining consequences of retinal membrane guanylyl cyclase (RetGC1) deficiency in human Leber congenital amaurosis en route to therapy: residual cone-photoreceptor vision correlates with biochemical properties of the mutants. *Hum Mol Genet*. 2013; 22:168–1883.
35. Jacobson SG, Aleman TS, Cideciyan AV, et al. Human cone photoreceptor dependence on RPE65 isomerase. *Proc Natl Acad Sci U S A*. 2007;104:15123–15128.
36. Aleman TS, Cideciyan AV, Sumaroka A, et al. Inner retinal abnormalities in X-linked retinitis pigmentosa with RPGR mutations. *Invest Ophthalmol Vis Sci*. 2007;48:4759–4765.
37. Aleman TS, Cideciyan AV, Sumaroka A, et al. Retinal laminar architecture in human retinitis pigmentosa caused by Rhodopsin gene mutations. *Invest Ophthalmol Vis Sci*. 2008;49: 1580–1590.
38. Carroll J, Baraas RC, Wagner-Schuman M, et al. Cone photoreceptor mosaic disruption associated with Cys203Arg mutation in the M-cone opsin. *Proc Natl Acad Sci U S A*. 2009; 106:20948–20953.
39. Rangaswamy NV, Patel HM, Locke KG, Hood DC, Birch DG. A comparison of visual field sensitivity to photoreceptor thickness in retinitis pigmentosa. *Invest Ophthalmol Vis Sci*. 2010;51:4213–4219.
40. Ooto S, Hangai M, Tomidokoro A, et al. Effects of age, sex, and axial length on the three-dimensional profile of normal macular layer structures. *Invest Ophthalmol Vis Sci*. 2011; 52:8769–8779.
41. Chui TY, Song H, Clark CA, Papay JA, Burns SA, Elsner AE. Cone photoreceptor packing density and the outer nuclear layer thickness in healthy subjects. *Invest Ophthalmol Vis Sci*. 2012;53:3545–3553.
42. Sung KR, Wollstein G, Bilonick RA, et al. Effects of age on optical coherence tomography measurements of healthy retinal nerve fiber layer, macula, and optic nerve head. *Ophthalmology*. 2009;116:1119–1124.
43. Milam AH, Li ZY, Fariss RN. Histopathology of the human retina in retinitis pigmentosa. *Prog Retin Eye Res*. 1998;17; 175–205.
44. Machida S, Kondo M, Jamison JA, et al. P23H rhodopsin transgenic rat: correlation of retinal function with histopathology. *Invest Ophthalmol Vis Sci*. 2000;41:3200–3209.
45. Sarks JP, Sarks SH, Killingsworth MC. Evolution of soft drusen in age-related macular degeneration. *Eye (Lond)*. 1994;8:269–283.
46. Johnson PT, Lewis GP, Talaga KC, et al. Drusen-associated degeneration in the retina. *Invest Ophthalmol Vis Sci*. 2003; 44:4481–4488.
47. Johnson PT, Brown MN, Pulliam BC, Anderson DH, Johnson LV. Synaptic pathology, altered gene expression, and degeneration in photoreceptors impacted by drusen. *Invest Ophthalmol Vis Sci*. 2005;46:4788–4795.
48. Gass JD. Drusen and disciform macular detachment and degeneration. *Arch Ophthalmol*. 1973;90:206–217.
49. Bressler NM, Munoz B, Maguire MG, et al. Five-year incidence and disappearance of drusen and retinal pigment epithelial abnormalities. Waterman study. *Arch Ophthalmol*. 1995;113: 301–308.
50. Smith RT, Sohrab MA, Pumariega N, et al. Dynamic soft drusen remodelling in age-related macular degeneration. *Br J Ophthalmol*. 2010;94:1618–1623.
51. Yehoshua Z, Wang F, Rosenfeld PJ, Penha FM, Feuer WJ, Gregori G. Natural history of drusen morphology in age-related macular degeneration using spectral domain optical coherence tomography. *Ophthalmology*. 2011;118:2434–2441.
52. Doyle SL, Campbell M, Ozaki E, et al. NLRP3 has a protective role in age-related macular degeneration through the induction of IL-18 by drusen components. *Nat Med*. 2012;18:791–798.
53. Schmitz-Valckenberg S, Fleckenstein M, Helb HM, Charbel Issa P, Scholl HP, Holz FG. In vivo imaging of foveal sparing in geographic atrophy secondary to age-related macular degeneration. *Invest Ophthalmol Vis Sci*. 2009;50:3915–3921.
54. Tackenberg MA, Tucker BA, Swift JS, et al. Muller cell activation, proliferation and migration following laser injury. *Mol Vis*. 2009;15:1886–1896.
55. Faktorovich EG, Steinberg RH, Yasumura D, Matthes MT, LaVail MM. Photoreceptor degeneration in inherited retinal dystrophy delayed by basic fibroblast growth factor. *Nature*. 1990; 347:83–86.
56. Faktorovich EG, Steinberg RH, Yasumura D, Matthes MT, LaVail MM. Basic fibroblast growth factor and local injury protect photoreceptors from light damage in the rat. *J Neurosci*. 1992; 12:3554–3567.
57. Wen R, Song Y, Cheng T, et al. Injury-induced upregulation of bFGF and CNTF mRNAS in the rat retina. *J Neurosci*. 1995;15: 7377–7385.
58. Xiao M, Sastry SM, Li ZY, et al. Effects of retinal laser photocoagulation on photoreceptor basic fibroblast growth factor and survival. *Invest Ophthalmol Vis Sci*. 1998;39:618–630.
59. Tuo J, Grob S, Zhang K, Chan CC. Genetics of immunological and inflammatory components in age-related macular degeneration. *Ocul Immunol Inflamm*. 2012;20:27–36.
60. Sunness JS, Johnson MA, Massof RW, Marcus S. Retinal sensitivity over drusen and nondrusen areas. A study using fundus perimetry. *Arch Ophthalmol*. 1988;106:1081–1084.
61. Takamine Y, Shiraki K, Moriwaki M, Yasunari T, Miki T. Retinal sensitivity measurement over drusen using scanning laser ophthalmoscope microperimetry. *Graefes Arch Clin Exp Ophthalmol*. 1998;236:285–290.
62. Midena E, Vujosevic S, Convento E, Manfre' A, Cavarzeran F, Pilotto E. Microperimetry and fundus autofluorescence in patients with early age-related macular degeneration. *Br J Ophthalmol*. 2007;91:1499–1503.
63. Hartmann KI, Bartsch DU, Cheng L, et al. Scanning laser ophthalmoscope imaging stabilized microperimetry in dry age-related macular degeneration. *Retina*. 2011;31:1323–1331.